New Journal of Physics
An Institute of Physics and Deutsche Physikalische Gesellschaft Journal

Anisotropic dissipation of superfluid flow in a periodically dressed Bose–Einstein condensate

D M Stamper-Kurn
Department of Physics, University of California, Berkeley, CA 94720, USA
E-mail: dmsk@socrates.berkeley.edu

New Journal of Physics **5** (2003) 50.1–50.13 (http://www.njp.org/)
Received 15 November 2002
Published 30 May 2003

Abstract. The introduction of a steady-state spatially periodic Raman coupling between two components of an ultracold atomic gas produces a dressed-state gas with an anisotropic and tunable dispersion relation. A Bose–Einstein condensate (BEC) formed in such a gas is consequently characterized by an anisotropic superfluid critical velocity. The anisotropic dissipation of superfluid flow is quantified by considering the scattering of impurities flowing through this superfluid. A gradual transition from the isotropic nature of an uncoupled BEC to the anisotropic periodically-dressed condensate is obtained as the strength of the Raman coupling is varied. These results present a clear signature for future experimental realizations of this novel superfluid.

Contents

PII: S1367-2630(03)56165-1

1. Introduction

The experimental attainment of quantum degenerate dilute gases, composed of both bosonic and fermionic atoms, has created many new opportunities in the study of quantum fluids. In particular, recent years have seen a flurry of experimental studies of superfluidity in dilute, scalar Bose–Einstein condensates (BECs). These include the observations of critical velocities for superfluid flow about microscopic [1] and macroscopic [2] obstacles, the onset of turbulent flow above this critical velocity [3], beautiful studies of quantized vortices and vortex lattices in rotating BECs [4]–[6] and other manifestations of irrotational superfluid flow [7, 8]. These experiments are closely analogous to those performed on another scalar superfluid, liquid ^{4}He, but apply new experimental probes and allow new insights due to the vastly different parameter regime of the dilute atomic gases, and their amenability to a new set of tools for manipulation and probing.

Dilute atomic gases also offer the opportunity to create novel quantum fluids by using these tools to manipulate the internal and external states of the atoms comprising the superfluid. For example, different types of multi-component condensates have been studied: externally coupled two-component condensates of ^{87}Rb at JILA (reviewed in [9]) and $F = 1$ spinor condensates of sodium at MIT (reviewed in [10]). One experiment at JILA explored how a spatially selective coupling between two trapped hyperfine levels of a rubidium condensate leads to a 'winding' of the order parameter, akin to the phase winding of the order parameter which occurs due to rotation about a vortex core, and how this winding is recurrently 'undone' due to the motional dynamics of a two-component condensate [11]. This observation shows that vortices in such a novel system should not be metastable (similarly predicted for spinor condensates [12]), a major modification from the superfluid behaviour of a single-component gas.

In a similar vein, we have previously considered the novel superfluid properties introduced into a two-component Bose condensed atomic gas which is coupled by a spatially periodic coupling field [13]. This spatially periodic coupling results from intersecting, non-collinear laser beams which induce a Raman coupling between two internal states of the ultracold gas. The Raman coupling introduces an anisotropy to this periodically-dressed fluid which should manifest itself in an anisotropic superfluid critical velocity. Controlling various parameters of the Raman coupling laser beams allows one to dramatically alter this critical velocity, leading to the dissipation of superfluid flow at velocities much lower than the critical velocity for the uncoupled Bose condensate.

In this paper, we develop further a theory describing the dissipation of superfluid flow in a periodically-dressed Bose–Einstein condensate (PDBEC). Using the Bogoliubov approximation theory which was introduced in [13], the possible dissipation of superfluid flow is treated by analysing the scattering of massive impurities which flow through the superfluid. In analogy with similar calculations for a scalar BEC [1, 14, 15], impurity scattering at low impurity velocities is found to be suppressed by the energetics of the quasiparticle spectrum (related to the Landau criterion for superfluidity [16]), by the suppression of density fluctuations in the low-momentum phonon regime [17] and by variations of the internal-state compositions of quasiparticles at different wavevectors. These effects combine to give a smooth evolution in the dissipation rates for superfluid flow as the Raman coupling strength is increased, gradually converting an uncoupled two-component BEC (essentially a scalar superfluid) to a periodically-dressed condensate with dramatically different superfluid properties. This superfluid dissipation rate gives an appealingly clear signature for future experimental studies.

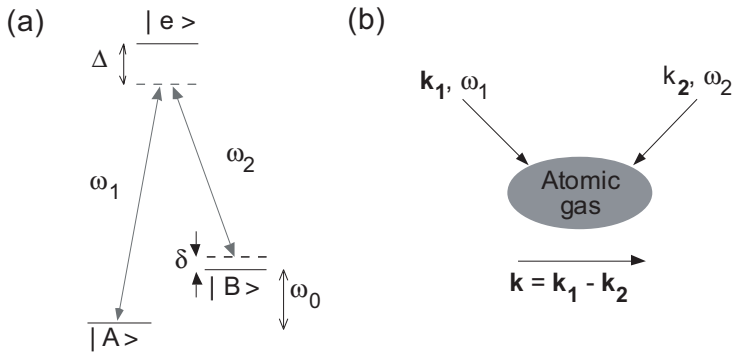

Figure 1. Engineering properties of a periodically-dressed atomic gas. (a) Laser beams of frequency ω_1 and ω_2 induce Raman transitions between internal states $|A\rangle$ and $|B\rangle$. The beams share a common large detuning Δ from the excited atomic state, and this state is adiabatically eliminated in the theoretical treatment. The lasers are detuned by an amount δ from the two-photon Raman transition. (b) Such a Raman transition imparts a momentum transfer of $\hbar\boldsymbol{k} = \hbar(\boldsymbol{k}_1 - \boldsymbol{k}_2)$, where $\boldsymbol{k}_1$ and $\boldsymbol{k}_2$ are the wavevectors of the Raman coupling lasers.

2. Quasiparticle modes of the periodically-dressed condensate

As presented in [13], a PDBEC is formed of atoms of mass m with two internal states, A and B, separated by an energy difference $\hbar\omega_0$. These atoms are exposed continuously to two laser beams of wavevectors $\boldsymbol{k}_1$ and $\boldsymbol{k}_2$ and frequencies ω_1 and ω_2, which couple the states A and B via a Raman transition (see figure 1). In such a Raman transition, an atom in internal state A with wavevector $\boldsymbol{q} - \boldsymbol{k}/2$ absorbs a photon from beam 1 and emits a photon into beam 2, arriving in internal state B with wavevector $\boldsymbol{q} + \boldsymbol{k}/2$ gaining a momentum $\hbar\boldsymbol{k} = \hbar(\boldsymbol{k}_1 - \boldsymbol{k}_2)$ and a kinetic energy $\hbar\delta = \hbar(\omega_1 - \omega_2 - \omega_0)$.

Keeping in mind this coupling between atoms of different momenta, we let a_q ($a_q^\dagger$) be the creation (annihilation) operator for an atom in internal state A and wavevector $\boldsymbol{q} - \boldsymbol{k}/2$, and similarly let b_q ($b_q^\dagger$) be the creation (annihilation) operator for an atom in internal state B and wavevector $\boldsymbol{q} + \boldsymbol{k}/2$. We refer to these as the bare-state creation and annihilation operators. The justification for this particular notation lies in the dressed-state picture [18], in which one considers the driving optical fields to be part of the quantum system. In this picture, the Raman transition connects the states $|a_q\rangle = |A, \boldsymbol{q} - \boldsymbol{k}/2; N_1+1, N_2\rangle$ and $|b_q\rangle = |B, \boldsymbol{q}+\boldsymbol{k}/2; N_1, N_2+1\rangle$, where $|a_q\rangle$ represents an atom in state A and wavevector $\boldsymbol{q} - \boldsymbol{k}/2$ and an optical field with $N_1 + 1$ photons in beam 1 and N_2 photons in beam 2, and similarly for $|b_q\rangle$. In the dressed-state picture, $|a_q\rangle$ and $|b_q\rangle$ are states for which the total momentum of the atom + photon system is equal—by a proper choice of inertial frame, this total momentum is taken to be $\hbar\boldsymbol{q}$. The states are separated by an energy difference $\hbar\delta$, and coupled by a static and (in the dressed-state picture) spatially uniform Raman coupling. The system is then represented by a many-body Hamiltonian of the form

$$\mathcal{H} = \sum_{\boldsymbol{q}} \left[\left(\frac{\hbar^2}{2m} \left(\boldsymbol{q} - \frac{\boldsymbol{k}}{2} \right)^2 + \frac{\hbar\delta}{2} \right) a_q^\dagger a_q + \left(\frac{\hbar^2}{2m} \left(\boldsymbol{q} + \frac{\boldsymbol{k}}{2} \right)^2 - \frac{\hbar\delta}{2} \right) b_q^\dagger b_q + \frac{\hbar\Omega}{2} \left(b_q^\dagger a_q + a_q^\dagger b_q \right) \right]. \tag{1}$$

Here Ω is the two-photon Rabi frequency characterizing the strength of the Raman transition, determined by the polarizations and intensities of the driving laser beams and by dipole matrix elements of the atoms.

This Hamiltonian is diagonalized by transforming to the dressed-state creation and annihilation operators μ_q, $\mu_q^\dagger$, π_q, $\pi_q^\dagger$ which are defined as linear combinations of the bare-state operators:

$$\begin{pmatrix} a_q \\ b_q \end{pmatrix} = \begin{pmatrix} \cos\theta_q/2 & \sin\theta_q/2 \\ -\sin\theta_q/2 & \cos\theta_q/2 \end{pmatrix} \begin{pmatrix} \mu_q \\ \pi_q \end{pmatrix}. \tag{2}$$

The mixing angle θ_q is defined by the relation $\tan\theta_q = \omega/(\delta - \hbar \boldsymbol{q}\cdot\boldsymbol{k}/m)$. The dressed states have energies

$$\hbar\omega_q^{\pm} = \frac{\hbar^2}{2m}\left(q^2 + \frac{k^2}{4}\right) \pm \frac{\hbar}{2}\sqrt{\left(\delta - \frac{\hbar \boldsymbol{q}\cdot\boldsymbol{k}}{m}\right)^2 + \Omega^2}. \tag{3}$$

Here, the minus sign refers to the lower dressed-state dispersion curve and to the operators μ_q and $\mu_q^\dagger$, while the plus sign refers to the upper dressed-state dispersion curve and to the operators π_q and $\pi_q^\dagger$.

A BEC formed from this periodically-dressed atomic gas has a macroscopic population of N_0 atoms in the lowest energy momentum state: this state lies on the lower dressed-state dispersion curve and is taken to have momentum $\hbar\boldsymbol{Q}$[1]. In [13], a Bogoliubov approximation theory was developed to account for the effects of weak interatomic interactions on a PDBEC. An interaction Hamiltonian of the form $\mathcal{H}_{\rm int} = \frac{g}{2}\sum_q (n_q n_{-q} - N)$ was considered, where N is the total number of atoms in the system and $n_q = \sum_k (a_{k+q}^\dagger a_k + b_{k+q}^\dagger b_k)$ is the Fourier transform of the density operator. Quasiparticle energies and operators were found by diagonalizing a 4×4 matrix $(H_q)_{ij} = (\mathcal{E}_q)_{ij} + \mu x_i x_j$, where $\mathcal{E}_q$ is a diagonal matrix with entries $(\mathcal{E}_q^-, -\mathcal{E}_{-q}^-, \mathcal{E}_q^+, -\mathcal{E}_{-q}^+)$ with $\mathcal{E}_q^\pm = \hbar(\omega_{Q+q}^\pm - \omega_Q^-)$, $\mu = gN$ is the chemical potential, and $x = (\cos\Delta_q, -\mathrm{i}\cos\Delta_{-q}, \sin\Delta_q, -\mathrm{i}\sin\Delta_{-q})$, where $\Delta_q = (\theta_{Q+q} - \theta_Q)/2$. Diagonalization yields

$$H_q = M_q \tilde{H}_q M_q^{-1} \tag{4}$$

where $\tilde{H}_q$ is a diagonal matrix with entries $\hbar(\tilde{\omega}_{Q+q}^-, -\tilde{\omega}_{Q-q}^-, \tilde{\omega}_{Q+q}^+, -\tilde{\omega}_{Q-q}^+)$ by which the lower (minus sign) and upper (plus sign) quasiparticle energies $\hbar\tilde{\omega}_{Q+q}^\pm$ are defined. One also obtains the creation and annihilation operators for the lower $(\tilde{\mu}_q, \tilde{\mu}_q^\dagger)$ and upper $(\tilde{\pi}_q, \tilde{\pi}_q^\dagger)$ branch quasiparticles through the following relation:

$$\begin{pmatrix} a_{Q+q} \\ \mathrm{i}a_{Q-q}^\dagger \\ b_{Q+q} \\ \mathrm{i}b_{Q-q}^\dagger \end{pmatrix} = R_q \begin{pmatrix} \mu_{Q+q} \\ \mathrm{i}\mu_{Q-q}^\dagger \\ \pi_{Q+q} \\ \mathrm{i}\pi_{Q-q}^\dagger \end{pmatrix} = R_q M_q \begin{pmatrix} \tilde{\mu}_{Q+q} \\ \mathrm{i}\tilde{\mu}_{Q-q}^\dagger \\ \tilde{\pi}_{Q+q} \\ \mathrm{i}\tilde{\pi}_{Q-q}^\dagger \end{pmatrix}. \tag{5}$$

[1] We do not consider here the possibility of a degenerate or near-degenerate ground state. Proper treatment of a PDBEC for such a situation requires a many-body treatment beyond the Bogoliubov approximation, as will be discussed elsewhere.

Here R_q contains trigonometric functions of $\theta_{Q+q}/2$ and $\theta_{Q-q}/2$ in accordance with equation (2). The Bose commutation relations take the form

$$[\chi_i, \chi_j^\dagger] = A_{ij} = \begin{cases} 0 & i \neq j \\ 1 & i = j = 1 \text{ or } i = j = 3 \\ -1 & i = j = 2 \text{ or } i = j = 4 \end{cases} \tag{6}$$

where χ represents any of the four-component vectors in equation (5). These relations are clearly preserved by the rotation matrix, i.e. $R_q A R_q^\dagger = A$, while the imposition of Bose commutation relations for the quasiparticle operators enforces a normalization criterion $M_q A M_q^\dagger = A$.

Experimentally, values for the Raman detuning δ, the Rabi frequency Ω, the chemical potential μ and the Raman momentum transfer $\hbar k$ can be chosen over a wide range of parameters. For example, let us consider a particular realization of a PDBEC using two hyperfine states of ^{87}Rb. One may consider the case of Raman excitation using two lasers both tuned near the $D2$ optical transition at a wavelength $\lambda \simeq 780$ nm. Thus, the Raman recoil energy $E_k = \hbar^2 k^2/2m$ can be readily tuned in the range $0 \leq E_k \leq h \times 15$ kHz. Properties of a PDBEC are governed by the ratios $\hbar\delta/E_k$, Ω/E_k and μ/E_k. The Raman detuning δ and the Rabi frequency Ω can be chosen nearly arbitrarily, reaching maximum values which are orders of magnitude larger than E_k. The chemical potential $\mu = 4\pi\hbar^2 an/m$ has a typical value of 1 kHz for a density of $n \simeq 1 \times 10^{14}$ cm^{-3} and a scattering length $a \simeq 100$ Bohr—thus the ratio μ/E_k can be as small as $\sim 1/10$ for counter-propagating Raman excitation lasers, and greatly increased by using Raman beams intersecting at small angles.

For illustration, we show in figure 2 the quasiparticle dispersion relations for a PDBEC with a chemical potential $\mu/E_k = 1$, a Raman detuning of $\hbar\delta/E_k = 1/2$ and Raman coupling strength $\hbar\Omega/E_k$ varying between 0 and 2. For this case of $\delta > 0$, a condensate is formed in the $\boldsymbol{Q} \simeq -\boldsymbol{k}/2$ state of the lower dispersion relation. In the absence of Raman coupling, this equality is exact, and the condensate is formed in the $|B\rangle$ internal state. Quasiparticle excitations in the $|B\rangle$ state follow the standard Bogoliubov result, while quasiparticles in state $|A\rangle$ have a free-particle dispersion relation—this can be thought of as due to the lack of a spatial interference term between the condensate and excitations in the $|A\rangle$ state at any wavevector. For small Rabi coupling strengths, one speaks more properly of excitations in the lower and upper quasiparticle dispersion relations, although the energies and internal-state compositions of these states remain relatively unchanged for wavevectors $\boldsymbol{q}$ far from the Doppler-shifted Raman resonance condition $\delta - \boldsymbol{q}\cdot\boldsymbol{k}/m = 0$. The lower quasiparticle dispersion relation has a local minimum near $\boldsymbol{q} = \boldsymbol{k}/2$ caused by the minimum of the dispersion relation for the bare $|A\rangle$ state atoms. By analogy to the roton minimum in the excitation spectrum of superfluid ^{4}He [17], we denote this feature as an 'artificial roton', although we mean to suggest no similarity between the specific structure of a roton and the plane-wave excitations of a PDBEC. As the Rabi frequency is increased further, a greater mixing of the internal state composition of the Bose condensate and the quasiparticle excitations occurs, and energy levels are shifted. In particular, the energy of the 'artificial roton' is shifted upwards due to interactions as the internal state composition of the Bose condensate and these excitations becomes more similar.

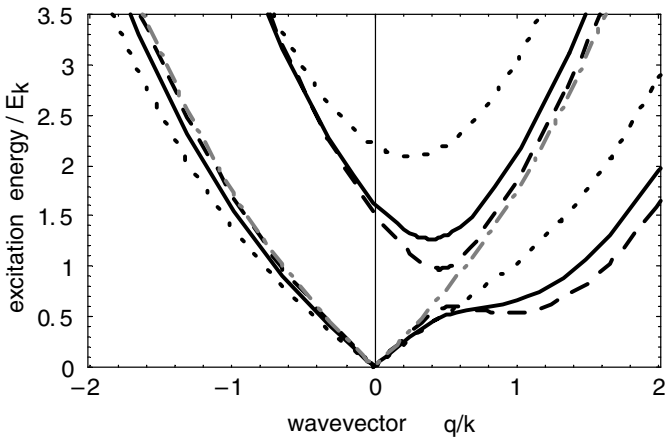

Figure 2. Quasiparticle dispersion relations for a PDBEC. Shown are quasiparticle energies in the lower (created by μ_{Q+q}) and upper (created by π_{Q+q}) dispersion curves with momentum $\boldsymbol{q}$ with respect to the condensate. Excitations parallel to the Raman momentum transfer are considered, with the definition $q = \boldsymbol{q} \cdot \boldsymbol{k}/k$. Black curves represent PDBECs with $\hbar\delta/E_k = 1/2$, $\mu/E_k = 1$ and $\hbar\Omega/E_k = 1/2$ (broken), 1 (dotted) and 2 (full). The grey chain curve shows the Bogoliubov excitation spectrum for a single-component condensate with $\mu/E_k = 1$.

3. Impurity scattering

We now consider the scattering of impurities passing through a uniform PDBEC. We consider impurities of mass M_c which have a free-particle dispersion relation $E_c = \hbar^2 k_c^2/2M_c$, where k_c is the impurity wavevector. Such impurities interact with the two components of the periodically-dressed condensate through an interaction of the form

$$\mathcal{H}_{\text{scat}} = \lambda \sum_{m,l,q} (a^\dagger_{m+q} a_m c^\dagger_{l+q} c_l + b^\dagger_{m+q} b_m c^\dagger_{l+q} c_l). \tag{7}$$

Here a_q, $a_q^\dagger$, b_q and $b_q^\dagger$ are defined as above, and c_q and $c_q^\dagger$ are the creation and annihilation operators, respectively, for the impurity particles. The coupling strength for the impurity scattering is λ, which we parametrize as $\lambda = 2\pi\hbar^2 a_c/M'$. This parametrization correctly describes low-energy s-wave scattering with a scattering length of a_c and the reduced mass $M' = mM/(m + M)$. Note that we have made the assumption that the scattering strengths between the impurity and atoms in states A and B are equal, and assume further that state changing collisions do not occur (the impurity is considered 'non-magnetic'). We may consider also the limit as the impurity mass becomes infinite while the impurity velocity $\boldsymbol{v} = \hbar\boldsymbol{k}/m$ remains constant ($\boldsymbol{k}$ is the impurity wavevector). We thereby obtain a description of the PDBEC flowing past a rigid obstacle with a velocity $\boldsymbol{v}$, and the concept of impurity scattering is replaced by the dissipation of superfluid flow.

The scattering rate of these impurities can be calculated using a perturbative approach as follows [14, 15]. We consider the system to be initially in the state $|0\rangle_{AB}|\boldsymbol{k}\rangle_C$, i.e. a PDBEC

with no excitations, and a single impurity particle of wavevector $\boldsymbol{k}$. The scattering Hamiltonian of equation (7) may couple this state to the final state $|f\rangle_{AB}|\boldsymbol{k}-\boldsymbol{q}\rangle_C$ in which the periodically-dressed gas is in the state $|f\rangle$ and the impurity wavevector changes from $\boldsymbol{k}$ to $\boldsymbol{k}-\boldsymbol{q}$. The matrix element for this transition is $\lambda\langle f|n_q|0\rangle$, where n_q is described above, and where the AB subscript labelling the quantum states of the periodically-dressed gas has been dropped. We then obtain the rate of impurity scattering by summing over all final states $|f\rangle$ and momentum transfers $\boldsymbol{q}$ using Fermi's golden rule.

We now make use of the Bogoliubov approximation. If we consider only weak scattering, we may restrict the final states to those containing a single quasiparticle, i.e. $|f\rangle = |\boldsymbol{q}^{\pm}\rangle$, where $|\boldsymbol{q}^{-}\rangle = \tilde{\mu}^{\dagger}_{Q+q}|0\rangle$ and $|\boldsymbol{q}^{+}\rangle = \tilde{\pi}^{\dagger}_{Q+q}|0\rangle$. The rate of impurity scattering is then

$$\Gamma = \frac{2\pi}{\hbar^2}\lambda^2 \sum_{q}\left[S_\mu(\boldsymbol{q})\delta\left(\tilde{\omega}^{-}_{Q+q} - \boldsymbol{v}\cdot\boldsymbol{q} + \frac{\hbar q^2}{2M_C}\right) + S_\pi(\boldsymbol{q})\delta\left(\tilde{\omega}^{+}_{Q+q} - \boldsymbol{v}\cdot\boldsymbol{q} + \frac{\hbar q^2}{2M_C}\right)\right] \tag{8}$$

where $\boldsymbol{v} = \hbar\boldsymbol{k}/M$ is the impurity velocity. We have introduced the quantities $S_\mu(\boldsymbol{q})$ and $S_\pi(\boldsymbol{q})$ which relate to the static structure factor describing density–density correlations in the Bose condensate. For a single-component BEC, the static structure factor $S(\boldsymbol{q})$ has been evaluated and measured [19, 20, 21]. For the PDBEC, we separate the contributions of the lower and upper excitation spectra as

$$S_\mu(\boldsymbol{q}) = \frac{1}{N_0}\langle 0|n_{-q}|\boldsymbol{q}^{-}\rangle\langle\boldsymbol{q}^{-}|n_q|0\rangle \tag{9}$$

$$S_\pi(\boldsymbol{q}) = \frac{1}{N_0}\langle 0|n_{-q}|\boldsymbol{q}^{+}\rangle\langle\boldsymbol{q}^{+}|n_q|0\rangle. \tag{10}$$

Physically, these quantities describe two effects. First, the magnitude of S_μ and S_π describes the contributions of quasiparticles in the lower (μ) or upper (π) quasiparticle state to density fluctuations (as opposed to phase fluctuations, which dominate, for example, for phonon excitations of a scalar Bose condensate [19, 20, 22]). Second, these quantities describe the degree to which the internal state composition of the condensate matches that of the quasiparticle. For instance, a condensate which is predominantly in the $|B\rangle$ internal state will not scatter strongly into quasiparticle states in which the $|A\rangle$ internal state is dominant, and thus the structure factor describing this scattering will be small.

Before proceeding to a calculation of S_μ and S_π, it is useful to consider the scattering rate Γ_0 for an ideal-gas, single-component BEC as the target gas. In this case, we may conveniently take $S_\mu(\boldsymbol{q}) = 1$, $S_\pi(\boldsymbol{q}) = 0$ and $\tilde{\omega}^{-}_{q} = \hbar q^2/2m$. Replacing $\sum_q = V/(2\pi)^3\int \mathrm{d}^3\boldsymbol{q}$, and substituting for λ we evaluate equation (8) and obtain simply

$$\Gamma_0 = \frac{\lambda^2 N_0 V M'^2 v}{\pi\hbar^4} = \frac{N_0}{V}\times 4\pi a_c^2 \times v, \tag{11}$$

i.e. the conventional expression for the scattering rate where N_0/V is the density of the target gas and $4\pi a_c^2$ is the collision cross section. We may then determine the impurity scattering rate in a PDBEC relative to that in an ideal gas, $F_{\mathrm{tot}} = \Gamma/\Gamma_0 = F_\mu + F_\pi$:

$$F_\mu = \frac{\hbar^2}{4\pi v M'^2}\int \mathrm{d}^3\boldsymbol{q}\, S_\mu(\boldsymbol{q})\delta\left(\tilde{\omega}^{-}_{Q+q} + \frac{\hbar q^2}{2M_C} - \boldsymbol{v}\cdot\boldsymbol{q}\right) \tag{12}$$

$$F_\pi = \frac{\hbar^2}{4\pi v M'^2}\int \mathrm{d}^3\boldsymbol{q}\, S_\pi(\boldsymbol{q})\delta\left(\tilde{\omega}^{+}_{Q+q} + \frac{\hbar q^2}{2M_C} - \boldsymbol{v}\cdot\boldsymbol{q}\right). \tag{13}$$

4. Structure factor formalism

To calculate the structure factors S_μ and S_π we start by expressing the density operator n_q in terms of the quasiparticle operators:

$$\begin{aligned} n_q &= \tfrac{1}{2}\sum_m (a^\dagger_{Q+m+q} - \mathrm{i}a_{Q-m-q}b^\dagger_{Q+m+q} - \mathrm{i}b_{Q-m-q}) \begin{pmatrix} a_{Q+m} \\ \mathrm{i}a^\dagger_{Q-m} \\ b_{Q+m} \\ \mathrm{i}b^\dagger_{Q-m} \end{pmatrix} \\ &= \tfrac{1}{2}\sum_m (\tilde{\mu}^\dagger_{Q+m+q} - \mathrm{i}\tilde{\mu}_{Q-m-q}\tilde{\pi}^\dagger_{Q+m+q} - \mathrm{i}\tilde{\pi}_{Q-m-q}) \\ &\quad \times M^\dagger_{q+m}R^\dagger_{q+m}R_m M_m \begin{pmatrix} \tilde{\mu}_{Q+m} \\ \mathrm{i}\tilde{\mu}^\dagger_{Q-m} \\ \tilde{\pi}_{Q+m} \\ \mathrm{i}\tilde{\pi}^\dagger_{Q-m} \end{pmatrix}. \end{aligned} \tag{14}$$

Acting on a PDBEC, the only important terms in the sum are those which include the condensate operators $\tilde{\mu}_Q$ and $\tilde{\mu}^\dagger_Q$. Applying the relations $\tilde{\mu}_{Q+q}|0\rangle = \tilde{\pi}_{Q+q}|0\rangle = 0$ for $\boldsymbol{q} \neq 0$, and the relation $M_{\mathbf{0}} = \mathbf{1}$, we define matrices $\alpha = M^\dagger_q R^\dagger_q R_{\mathbf{0}}$ and $\beta = R^\dagger_{\mathbf{0}} R_{-q} M_{-q}$ and obtain

$$n_q|0\rangle = \frac{\sqrt{N_0}}{2}((\alpha_{11} + \mathrm{i}\alpha_{12} + \mathrm{i}\beta_{12} + \beta_{22})\tilde{\mu}^\dagger_q|0\rangle + (\alpha_{31} + \mathrm{i}\alpha_{32} + \mathrm{i}\beta_{14} + \beta_{24})\tilde{\pi}^\dagger_q|0\rangle). \tag{15}$$

So

$$S_\mu(\boldsymbol{q}) = \tfrac{1}{4}|\alpha_{11} + \mathrm{i}\alpha_{12} + \mathrm{i}\beta_{12} + \beta_{22}|^2 \tag{16}$$

$$S_\pi(\boldsymbol{q}) = \tfrac{1}{4}|\alpha_{31} + \mathrm{i}\alpha_{32} + \mathrm{i}\beta_{14} + \beta_{24}|^2. \tag{17}$$

The static structure factors $S_\mu(\boldsymbol{q})$ and $S_\pi(\boldsymbol{q})$ for a PDBEC are shown in figures 3 and 4. The specific values for the Raman detuning δ, the Rabi frequency Ω and the chemical potential μ are relevant for a particular realization of a PDBEC using two hyperfine states of a ^{87}Rb, as discussed above. The division of the scattering weight between the lower (S_μ) and upper (S_π) quasiparticle branches can be understood by considering the composition of the dressed-state quasiparticles, which is related by equation (2) to the mixing angle θ_q. This angle ranges from $\theta_q = 0$ for $\boldsymbol{q}\cdot\boldsymbol{k} \to -\infty$ to $\theta_q = \pi$ for $\boldsymbol{q}\cdot\boldsymbol{k} \to +\infty$, reaching $\theta_q = \pi/2$ at the Doppler-shifted Raman resonance $\delta - \boldsymbol{q}\cdot\boldsymbol{k}/m = 0$. For small Rabi frequency, θ_q, and hence the internal state composition of the dressed states varies rapidly about the Raman resonance condition, while for large Rabi frequency, this variation occurs over a broader range of q. This behaviour is reflected in the structure factors, as illustrated by figure 3. By continuity, the internal state composition of the condensate in the μ_Q state is nearly identical to that of excitations in the lower quasiparticle branch (created by $\tilde{\mu}^\dagger_{Q+q}$), and nearly orthogonal to that of excitations in the upper quasiparticle branch (created by $\tilde{\pi}^\dagger_{Q+q}$). Thus, since elastic scattering from a 'non-magnetic' impurity does not affect the internal state distribution, $S_\pi(\boldsymbol{q}) \simeq 0$ generally for small q. Away from $q = 0$, the division of the scattering weight between the upper and lower quasiparticle branches depends on the strength of the Rabi coupling. For small Rabi frequencies, the scattering strength shifts abruptly from the lower to the upper quasiparticle branch at the Doppler-shifted Raman resonance. For large Rabi frequency, the changes in the scattering strengths are more gradual, with scattering into both branches showing a significant weight for a wide range about the Raman resonance

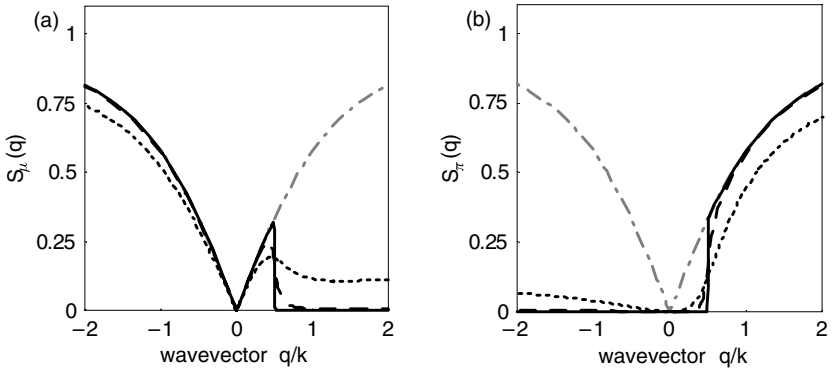

Figure 3. Variations of the static structure factors (a) $S_\mu(\boldsymbol{q})$ and (b) $S_\pi(\boldsymbol{q})$ with the Raman coupling strength Ω. The wavevector $\boldsymbol{q}$ is collinear with the Raman momentum transfer $\boldsymbol{k}$ with $q = \boldsymbol{q}\cdot\boldsymbol{k}/k$. Three black curves describe a PDBEC with $\hbar\delta/E_k = 1/2$, $\mu/E_k = 1$ and $\hbar\Omega/E_k = 0$ (full), 1/4 (broken) and 1 (dotted). Scattering for $q \sim 0$ and $q < 0$ occurs only into the lower quasiparticle branch and for $q \gg k$ into the upper quasiparticle branch. In other regions, stronger Raman coupling leads to eigenstates with mixed populations in the internal states $|A\rangle$ and $|B\rangle$ over a broader range of q, and thus impurity scattering occurs into both the lower and upper quasiparticle branches. Also shown is the structure factor $S(\boldsymbol{q})$ for a scalar BEC (grey chain curve) with $\mu/E_k = 1$.

condition. This variation is particularly relevant for the scattering of impurities near the Landau critical velocity, as discussed below.

As illustrated in figure 4, interatomic interactions suppress scattering at small momentum transfers. For a single-component homogeneous BEC, the structure factor $S(\boldsymbol{q}) = q^2/\sqrt{q^2(q^2+2\xi^{-2})}$ is small for wavevectors of magnitude $q < 1/\xi$, where $\xi = \sqrt{2m\mu/\hbar^2}$ is the healing length. Similarly, for the PDBEC, we find a suppression of the structure factors $S_\mu(\boldsymbol{q})$ and $S_\pi(\boldsymbol{q})$ for $q < k\sqrt{2\mu/E_k}$, as shown in the figure. This suppression of the structure factor in a PDBEC could be probed experimentally as it was for a scalar BEC by studying shallow-angle optical Bragg scattering [19, 20].

5. Dissipation of superfluid flow

Finally, let us use the formalism developed above to describe superfluid properties of a PDBEC. In [13], we applied the Landau criterion to determine the critical velocity for superfluidity in a PDBEC given the quasiparticle dispersion relations. This criterion gives the superfluid critical velocity along a direction $\hat{\boldsymbol{q}}$ as having a magnitude $v_c = \min_{q,i} E_i(q\hat{\boldsymbol{q}})/\hbar q$, where $E_i(\boldsymbol{q})$ are the energies of possible excitations with wavevector $\boldsymbol{q}$. Using the momentum definitions for a PDBEC, these would be the quasiparticle energies $\hbar\omega^{\pm}_{Q+q}$. In an unperturbed, single-component weakly interacting condensate, this critical velocity v_c^0 is equal to the Bogoliubov speed of sound $c_s = \sqrt{\mu/m}$ in all directions. In a PDBEC, the anisotropic quasiparticle dispersion relation leads directly to the prediction of an anisotropic superfluid critical velocity, and to the possibility of a critical velocity lower than that of the unperturbed condensate.

One may determine this critical velocity graphically by finding the line of minimum absolute

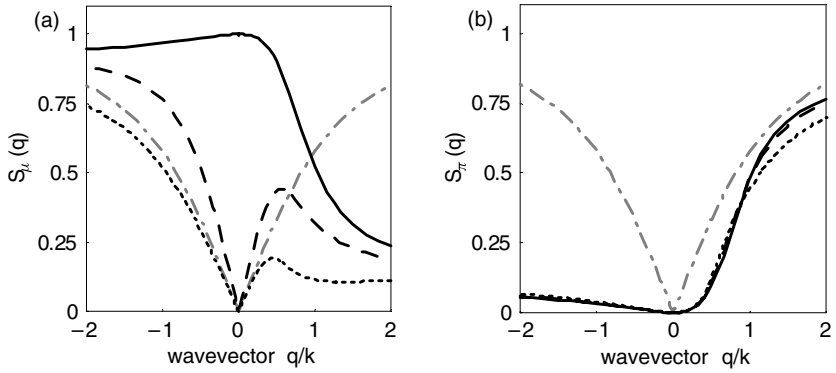

Figure 4. Static structure factor (a) $S_\mu(\boldsymbol{q})$ and (b) $S_\pi(\boldsymbol{q})$ for a PDBEC. The wavevector $\boldsymbol{q}$ is collinear with the Raman momentum transfer $\boldsymbol{k}$ with $q = \boldsymbol{q}\cdot\boldsymbol{k}/k$. Three black curves describe a PDBEC with $\hbar\delta/E_k = 1/2$, $\hbar\Omega/E_k = 1$ and $\mu/E_k = 0$ (full), 1/4 (broken) and 1 (dotted). The condensate in the μ_Q state is predominantly in the internal state B; thus, scattering predominantly occurs into the lower quasiparticle branch for $q < 0$ and into the upper quasiparticle branch for large $q > 0$. For $q \sim 0.5$ both $S_\mu(\boldsymbol{q})$ and $S_\pi(\boldsymbol{q})$ are significant since quasiparticles contain large fractions of both $|A\rangle$ and $|B\rangle$. Interactions suppress scattering at small momentum transfer, an effect seen also in the structure factor $S(\boldsymbol{q})$ for a scalar BEC (grey chain curve) with $\mu/E_k = 1$.

slope which connects the origin and the quasiparticle dispersion curve (see figure 2). For the PDBEC, the superfluid critical velocity may be suppressed by the presence of the 'artificial roton' feature in the lower dispersion curve. This suppression occurs in the direction of the Raman momentum transfer $\hbar\boldsymbol{k}$ for the case of $\delta > 0$ (as shown in the figure), or in the opposite direction for $\delta < 0$.

However, while the Landau criterion determines the minimum velocity for the dissipation of superfluid flow, it does not quantify the onset of such dissipation as the velocity is increased beyond the critical value. Indeed, for extremely weak Raman coupling, even though the superfluid critical velocity is strictly different, one should expect the fluid properties of a PDBEC to be nearly identical to that of a two-component BEC in the complete absence of Raman coupling. We can quantitatively assess this description using the formalism developed above for the determination of the matrix elements S_μ and S_π, and therefrom the normalized scattering rates F_μ and F_π.

The results of such calculations for infinitely massive impurities (i.e. superfluid flow about rigid obstacles) are presented in figures 5 and 6. Values of F_μ and F_π were determined by numerical integration in which the delta function in equations (12) and (13) was approximated by a narrow Gaussian distribution whose width was adjusted to give reasonable numerical convergence. As we expect, for small Rabi frequencies Ω the properties of a PDBEC are quite similar to those of an uncoupled two-component BEC. The scattering probability for impurity atoms (related to the viscosity of the fluid) is indeed non-zero at velocities lower than the superfluid critical velocity for the unperturbed gas, demonstrating that the critical velocity is suppressed along the direction of Raman scattering. This scattering at low velocities occurs through the excitation of quasiparticles near the local minimum (the 'artificial roton') in the

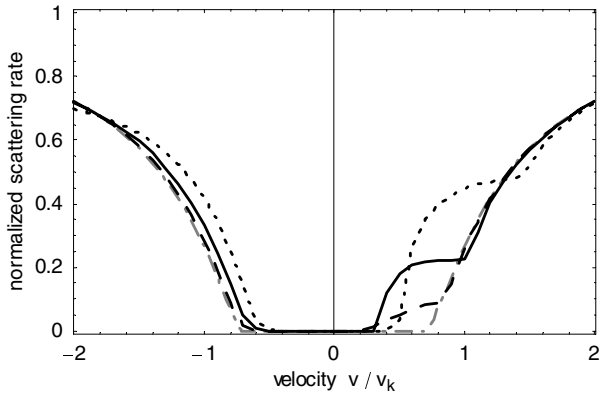

Figure 5. Dissipation strength of superfluid flow in periodically-dressed BECs. The scattering rate $F_{\rm tot}$ for infinitely massive impurities travelling through the condensate, normalized to the scattering in an ideal gas Bose condensate at similar densities, is plotted versus the velocity of the impurity. Velocities are parallel to the Raman momentum transfer, with $v = \boldsymbol{v} \cdot \boldsymbol{k}/k$ and $v_k = \hbar k/m$. Black curves show results for PDBECs with varying strengths of the Raman coupling; for all curves, $\delta/E_k = 1/2$ and $\mu/E_k = 1$ while $\hbar\omega/E_k = 1/2$ (broken), 1 (full) or 2 (dotted). The grey chain curve shows results for a one-component condensate with $\mu/E_k = 1$. The superfluid critical velocity of the PDBEC in the direction of the Raman momentum transfer is suppressed with respect to an uncoupled condensate. For weakly Raman coupling, the dissipation at low velocities is weak. This dissipation grows stronger as the Raman coupling strength is increased.

lower dispersion relation. However, this scattering channel is weak for small values of the Rabi frequency Ω, and thus the scattering strength $F_{\rm tot}$ remains weak until the curve joins that of the uncoupled condensate and the scattering strength is increased by phonon scattering.

The effects of increasing the Rabi frequency are two-fold. First, as Ω increases, the internal state composition of the 'artificial roton' excitation becomes more similar to the internal state composition of the BEC. This causes an increase in the scattering strength (as indicated also in the calculations of S_μ shown in figures 4 and 3). Simultaneously, because of this overlap of the internal state composition, the energy of these excitations is increased, approaching the energy given by the one-component Bogoliubov spectrum, albeit with an appropriately modified effective mass. Thus, the minimum velocity at which scattering occurs increases as the Rabi frequency increases. At moderate values of the Rabi frequency (where $\hbar\Omega/E_k \sim 1$), the scattering rate versus velocity has a two-step shape as scattering is first enhanced by strong scattering into the 'artificial roton' state, and then later enhanced by phonon scattering when the velocity is near v_c^0. As shown in figure 6 for one typical parameter setting, only F_μ contributes to the weak scattering at velocities smaller than v_c^0. At velocities greater than v_c^0, scattering into the upper dispersion curve is allowed and $F_\pi \neq 0$.

This two-step curve gives a clear signature which should be visible in experimental probes of superfluid flow. Indeed, experiments such as those performed by Chikkatur *et al* [1], in which atoms of another ground-state hyperfine level were used as scattering impurities in a dilute atomic Bose condensate, could be carried out in a straightforward manner. It would be interesting to consider further how other aspects of superfluidity, such as the onset of turbulent flow [2] or the

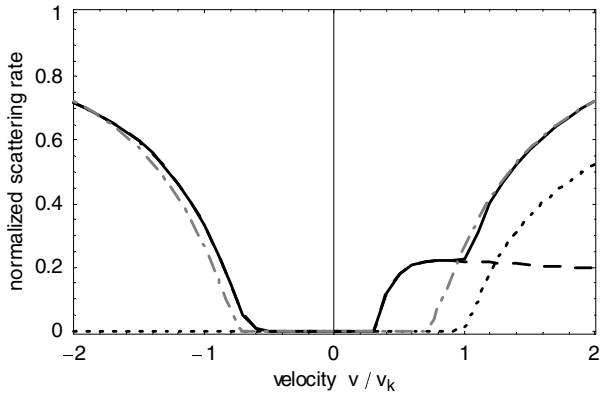

Figure 6. Normalized rates for production of lower (F_μ, broken curve) and upper (F_π, dotted curve) quasiparticle excitations due to scattering off infinitely massive impurities moving at velocities v in a PDBEC. Velocities are parallel to the Raman momentum transfer, with $v = \boldsymbol{v}\cdot\boldsymbol{k}/k$ and $v_k = \hbar k/m$. Black curves show results for a PDBEC with $\hbar\delta/E_k = 1/2$, $\mu/E_k = 1$ and $\hbar\Omega/E_k = 1$, with the full curve showing the total normalized scattering rate $F_{\rm tot}$. The grey chain curve shows the normalized scattering rate for a one-component condensate with $\mu/E_k = 1$. For $v > 0$ (for this case where $\delta > 0$), impurity scattering at low velocities is enhanced compared to the one-component condensate. This scattering leads to the creation of excitations in the lower dispersion curve ($F_\mu > 0$) around the 'artificial roton' feature in the quasiparticle dispersion relations. At velocities near the critical velocity for the unperturbed condensate, v_c^0, scattering is allowed into the upper dispersion relation $F_\pi > 0$, and the normalized scattering rate approaches that of a one-component condensate. For $v < 0$, energy and momentum conservation imply that only scattering into the lower quasiparticle excitations is allowed at the velocities considered.

metastability of quantized vortices [4, 5], are affected by the anisotropic nature of a PDBEC.

In conclusion, dissipation of superfluid motion in a PDBEC above the superfluid critical velocity was treated. A formalism was developed for the calculation of the static structure factors S_μ and S_π describing density–density correlations from quasiparticles in the lower (μ) and upper (π) excitation branches of the periodically-coupled gas. Following a perturbation theory approach, the scattering rate of massive impurities, or equivalently the damping rate of superfluid motion past microscopic obstacles, was calculated. Raman coupling of a two-component condensed gas leads to a suppression of the superfluid critical velocity. The impurity scattering rate evolves smoothly as the Raman coupling strength is increased. The superfluid damping is weak for weak Raman coupling, and becomes more significant as the Raman coupling strength is increased.

Acknowledgments

I thank James Higbie for insightful discussions. Support from the NSF, the Sloan Foundation, the Packard Foundation and the University of California Hellman Family Faculty Fund is gratefully acknowledged.

References

[1] Chikkatur A C *et al* 2000 *Phys. Rev. Lett.* **85** 483
[2] Raman C *et al* 1999 *Phys. Rev. Lett.* **83** 2502
[3] Onofrio R *et al* 2000 *Phys. Rev. Lett.* **85** 2228
[4] Matthews M R *et al* 1999 *Phys. Rev. Lett.* **83** 2498
[5] Madison K W, Chevy F, Wohlleben W and Dalibard J 2000 *Phys. Rev. Lett.* **84** 806
[6] Abo-Shaeer J R, Raman C, Vogels J M and Ketterle W 2001 *Science* **292** 476
[7] Marago O M *et al* 2000 *Phys. Rev. Lett.* **84** 2056
[8] Hechenblaikner G *et al* 2002 *Phys. Rev. Lett.* **88** 070406
[9] Cornell E A, Ensher J R and Wieman C E 1999 Bose–Einstein condensation in atomic gases *Proc. Int. School of Physics 'Enrico Fermi'* Course CXL, ed by M Inguscio, S Stringari and C E Wieman (Amsterdam: IOS Press) pp 15–66
[10] Stamper-Kurn D M and Ketterle W 2001 *Coherent Matter Waves* ed R Kaiser, C Westbrook and F David (New York: Springer) pp 137–218
[11] Matthews M R *et al* 1999 *Phys. Rev. Lett.* **83** 3358
[12] Ho T-L 1998 *Phys. Rev. Lett.* **81** 742
[13] Higbie J and Stamper-Kurn D M 2002 *Phys. Rev. Lett.* **88** 090401
[14] Ketterle W, Chikkatur A P and Raman C 2000 *Atomic Physics* vol 17, ed E Arimondo, P DeNatale and M Inguscio (Melville, NY: American Institute of Physics) pp 337–55
[15] Timmermans E and Cote R 1997 *Phys. Rev. Lett.* **80** 3419
[16] Landau L D 1941 *J. Phys.* (USSR) **5** 71
[17] Pines D and Nozières P 1999 *The Theory of Quantum Liquids* (Cambridge, MA: Perseus)
[18] Cohen-Tannoudji C, Dupont-Roc J and Grynberg G 1992 *Atom–Photon Interactions* (New York: Wiley)
[19] Stamper-Kurn D M *et al* 1999 *Phys. Rev. Lett.* **83** 2876
[20] Steinhauer J, Ozeri R, Katz N and Davidson N 2002 *Phys. Rev. Lett.* **88** 120407
[21] Zambelli F, Pitaevskii L, Stamper-Kurn D M and Stringari S 2000 *Phys. Rev.* A **61** 063608
[22] Dettmer S *et al* 2001 *Phys. Rev. Lett.* **87** 160406